Mon. Not. R. Astron. Soc. **292,** 63–70 (1997)

Hydrogen and carbon recombination lines towards the Galactic Centre near 328 MHz

D. Anish Roshi[1] and K. R. Anantharamaiah[2]

[1]*Radio Astronomy Centre, Tata Institute of Fundamental Research, PO Box 8, Ooty 643 001, India*
[2]*Raman Research Institute, Bangalore 560 080, India*

Accepted 1997 July 7. Received 1997 June 11; in original form 1997 February 10

ABSTRACT

We present observations of the H271α and the C271α recombination lines from nine positions around the Galactic Centre region made using the Ooty Radio Telescope. Both the lines were detected in emission in all the positions. In the integrated spectrum obtained by averaging over all the nine positions, the H271α line shows a narrow ($\sim$8 km s^{-1}) component superposed on a previously known broad ($\sim$38 km s^{-1}) component. Further observations are required to confirm the narrow feature. If the narrow component is real, then it could originate in a region with physical properties $T_e \sim 100$–1200 K, $n_e \sim 1.0$–1.5 cm^{-3} and EM$\sim$0.1–5.9 pc cm^{-6}. Both the broad and narrow components have similar non-zero LSR velocities, which suggests that the region responsible for the narrow component could be a partially ionized outer envelope of the low-density H II region in which the broad line originates.

The C271α line near 328 MHz appears to be the emission counterpart of the absorption lines observed in this direction near 75 MHz by Erickson, McConnell & Anantharamaiah. The phenomenon of turnover from absorption to emission of low-frequency carbon recombination lines is similar to that observed in the direction of Cas A by Payne, Anantharamaiah & Erickson. Using a model that incorporates the effects of dielectronic-like recombination in carbon, we show that the observed lines can be explained by a region with $T_e \sim 70$–80 K, $n_e \sim 0.005$–0.01 cm^{-3} and an effective pathlength of $\sim$200–500 pc. The filling factors, the neutral hydrogen densities and the thermal pressure deduced for these models are remarkably similar to the corresponding values for the cold neutral component (i.e. neutral H I clouds or CNM) of the interstellar medium. Thus our observations support the idea suggested by Anantharamaiah et al. and Payne et al. that the low-frequency carbon recombination lines arise in the neutral H I component of the ISM.

Key words: ISM: clouds – ISM: general – H II regions – Galaxy: centre – Galaxy: general – radio lines: ISM.

1 INTRODUCTION

Observations of low-frequency (< 500 MHz) recombination lines are sensitive to low-density ionized gas (Shaver 1975) and are therefore useful to investigate the physical properties of such regions. Towards the Galactic Centre, recombination lines have been detected over a wide range of frequencies – from 75 MHz (Erickson, McConnell & Anantharamaiah 1995) to 23 GHz (Rodriguez & Chaisson 1979). At high frequencies (> a few GHz), the recombination lines of hydrogen are dominated by emission from high-density ionized gas close to the Galactic Centre. The line emission often consists of many components with non-zero velocities and linewidths ranging from a few tens of km s^{-1} up to about $\sim$200 km s^{-1} (Anantharamaiah & Yusef-Zadeh 1988; Roelfsema & Goss 1992). The angular sizes of these regions are relatively small. However, at frequencies below 500 MHz only a feature near 0 km s^{-1} of width $\sim$35 km s^{-1} is dominant (Pedlar et al. 1978; Anantharamaiah & Bhattacharya 1986). The 0 km s^{-1} feature is believed to originate in ionized gas along the line of sight with physical parameters characteristic of low-density H II regions. Higher sensitivity observations near 328 MHz (Anantharamaiah & Bhattacharya 1986) do reveal weak non-zero velocity features (near -50 and $+30$ km s^{-1}) which may be related to the gas observed at higher frequencies. The lowest frequency at which a hydrogen recombination line has been detected towards the Galactic Centre is $\sim$145 MHz (Anantharamaiah, Payne & Bhattacharya 1990). Although it has been suggested that the region which emits the low-frequency lines is $\sim 2^\circ$ in extent, it is not clear whether it consists of a single cloud or a number of clouds along the line of sight.

While all the low-frequency hydrogen recombination lines towards the Galactic Centre have been detected only in emission, the carbon recombination lines have been detected both in emission and in absorption. The lines observed at frequencies above ~200 MHz were seen in emission (e.g. Pedlar et al. 1978) while observations at 75 MHz detected them in absorption (Anantharamaiah, Payne & Erickson 1988; Erickson et al. 1995). These lines are believed to originate in relatively cold ($T_e < 100$ K) interstellar clouds where hydrogen is largely neutral (in either atomic or molecular form) and gas-phase carbon is completely ionized by the background UV radiation. The physical properties and the angular extent of the line-emitting region are not well determined.

In this paper, we present observations of the H271α and the C271α recombination lines, which occur near 328 MHz, in the direction of the Galactic Centre. With the objective of determining the spatial structure of the line-emitting region, we observed nine positions around the Galactic Centre. These positions cover an angular span of ~1° along Galactic longitude and ~2° along Galactic latitude, centred at $l = 0°, b = 0°$. The integrated spectrum obtained by averaging the spectra of all the nine positions shows a hitherto unknown narrow (~8 km s^{-1}) hydrogen line feature in addition to the known relatively broad (~38 km s^{-1}) component. Further observations are required to confirm the narrow feature. Assuming that the narrow feature is real, we obtain constraints on the possible physical properties of the region responsible for this emission. The carbon lines detected in the present observations are used along with the available data at other frequencies to constrain the properties of the cloud emitting these lines. For the carbon lines, models that take into account the effects of dielectronic-like recombination (Watson, Western & Christensen 1980) for the computation of level populations are investigated in addition to those that use the hydrogenic approximation.

2 OBSERVATIONS AND RESULTS

We have observed nine positions around the Galactic Centre using the Ooty Radio Telescope (ORT). The coordinates of the observed positions are given in Table 1. The transitions observed were H271α (328.5959 MHz) and C271α (328.7597 MHz). The half-power beam of the telescope at the observed declination was 2° (in RA) × 6.2 arcmin (in Dec.). Each position was observed, on average, for about 13 h. A 512-channel one-bit autocorrelator with a bandwidth of 710 kHz was used for the observations. The velocity resolution was 2.1 km s^{-1}. Frequency switching was used to measure the reference spectra. The data were averaged after carefully editing those affected by interference.

Table 1. Coordinates of the observed positions ($b = 0.0$ for all the positions).

Position	l (°)	RA(2000) (h m s)	Dec.(2000) (° ′ ″)
1	0.4	17 46 34.15	−28 35 40.5
2	0.29	17 46 18.9	−28 41 18.9
3	0.18	17 46 02.86	−28 46 57.1
4	0.06	17 45 45.75	−28 53 06.0
5	359.94	17 45 28.6	−28 59 14.7
6	359.83	17 45 12.85	−29 04 52.6
7	359.71	17 44 55.64	−29 11 01.1
8	359.60	17 44 39.84	−29 16 38.7
9	359.48	17 44 22.56	−29 22 46.9

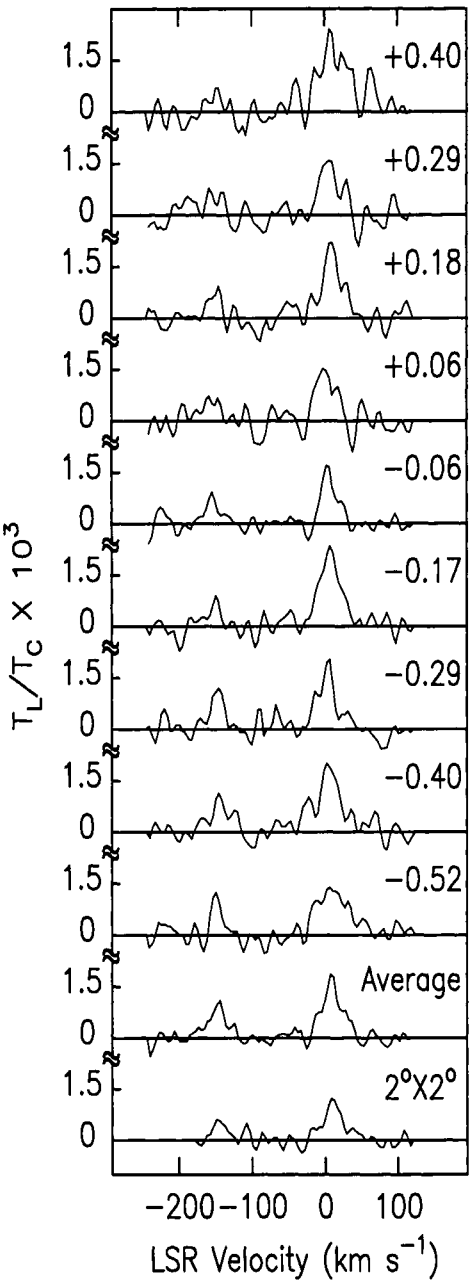

Figure 1. Recombination line spectra observed near 328 MHz towards nine positions around the Galactic Centre. The number next to each spectrum indicates the Galactic longitude. The bottom two plots show the average spectrum over the nine positions and the spectrum observed with a beam of 2° × 2° towards the Galactic Centre. The ordinate of the spectra is the line-to-continuum temperature ratio and the abscissa is the LSR velocity with respect to the H271α recombination line. The feature near −150 km s^{-1} corresponds to the C271α line.

The spectra from the nine positions are shown in Fig. 1. Hydrogen lines have been detected in all the nine positions and carbon lines in at least six of them. A spectrum obtained using a single module of the ORT which gives a resolution of 2° × 2° is also shown in Fig. 1. The line parameters, obtained from a single-component Gaussian fit to the spectra of the nine positions, are given in Table 2. The continuum antenna temperature (T_{AC}) measured at the nine positions with respect to an off-source position

Table 2. Parameters of the detected lines.

Position	H271α T_L/T_C $\times 10^3$	H271α ΔV (FWHM) (km s^{-1})	H271α V_{LSR} (km s^{-1})	C271α T_L/T_C $\times 10^4$	C271α ΔV (FWHM) (km s^{-1})	C271α V_{LSR} (km s^{-1})	T_{AC} (K)
1	1.9 ± 0.2	47.2 ± 6.3	$15.0^{+2.6}_{-8.6}$				602 ± 60.0
2	1.5 ± 0.2	33.5 ± 4.5	$9.3^{+1.7}_{-7.7}$				619 ± 62.0
3	2.0 ± 0.2	31.5 ± 3.6	$13.0^{+1.4}_{-7.4}$	8.6 ± 1.8	18.9 ± 4.9	$+2.8^{+2.0}_{-8.0}$	674 ± 67.0
4	1.5 ± 0.2	33.7 ± 4.5	$4.1^{+1.7}_{-7.7}$				841 ± 84.0
5	1.7 ± 0.2	20.2 ± 2.2	$7.4^{+0.9}_{-6.9}$	10.5 ± 0.7	12.3 ± 1.0	$-2.1^{+0.4}_{-6.4}$	1156 ± 116.0
6	2.2 ± 0.1	33.2 ± 1.5	$9.0^{+0.7}_{-6.7}$	11.0 ± 1.1	10.1 ± 1.2	$+3.1^{+0.5}_{-6.5}$	754 ± 75.0
7	1.8 ± 0.2	27.8 ± 3.0	$4.5^{+1.3}_{-7.3}$	13.4 ± 1.6	17.6 ± 2.7	$+5.6^{+1.0}_{-7.0}$	694 ± 69.0
8	1.7 ± 0.2	44.1 ± 4.7	$6.8^{+1.9}_{-7.9}$	12.9 ± 0.7	14.0 ± 0.9	$+7.0^{+0.4}_{-6.4}$	619 ± 62.0
9	1.3 ± 0.1	50.7 ± 4.4	$12.5^{+1.8}_{-7.8}$	14.8 ± 2.3	11.9 ± 2.1	$+2.3^{+0.9}_{-6.9}$	585 ± 59.0

Table 3. Parameters of the averaged profile.

Line	T_L/T_C $\times 10^3$	ΔV (FWHM) (km s^{-1})	V_{LSR} (km s^{-1})
H271α	0.82 ± 0.2	8.0 ± 2.3	$8.9^{+0.8}_{-6.8}$
	1.2 ± 0.2	37.7 ± 3.6	$9.3^{+1.1}_{-7.1}$
C271α	0.86 ± 0.07	17.5 ± 1.5	$3.1^{+0.7}_{-6.7}$

is also given in Table 2. For these measurements we have estimated the system temperature at the off-source position to be 150 K. After the observations were completed we discovered a possible offset of ~7 kHz in the first local oscillator frequency owing to an error in the frequency synthesizer. This would imply that the quoted LSR velocities could be systematically higher by ~6 km s^{-1}. This uncertainty is included in the errors quoted for the LSR velocities in Tables 2 and 3.

The spectrum at position 5 (Galactic Centre) is consistent, within the errors, with earlier observation of this position by Anantharamaiah & Bhattacharya (1986) using the ORT. The signal-to-noise ratio of the spectra is not sufficient to see the non-zero velocity features of the hydrogen line. We have averaged the spectra of all the nine positions; this average is also shown in Fig. 1. The averaged spectrum is equivalent to that observed with a beam of 1°× 2°. The non-zero features are not detected in this spectrum either. This is because the line intensity of these features gets beam-diluted, as demonstrated earlier by Pedlar et al. (1978) and Anantharamaiah & Bhattacharya (1986). The hydrogen feature in this spectrum shows a two-component structure – a narrow component (~8 km s^{-1}) superimposed on a broad (~38 km s^{-1}) component. While the broad feature is seen in all the earlier low-frequency observations, the narrow feature is observed for the first time.

3 THE HYDROGEN LINE

The large extent of the hydrogen line emitting region is evident from the detection of the line with similar line-to-continuum ratio at different positions around the Galactic Centre (Hart & Pedlar 1980) and in all the nine positions in the present observations, which cover ~1° in longitude. This is also evident from the detection of the hydrogen line with comparable line-to-continuum ratio with telescope beams of 3.°5 × 3.°5 (Casse & Shaver 1977), 1° × 2° (Anantharamaiah & Bhattacharya 1986) and 2° × 2° (see Fig. 1).

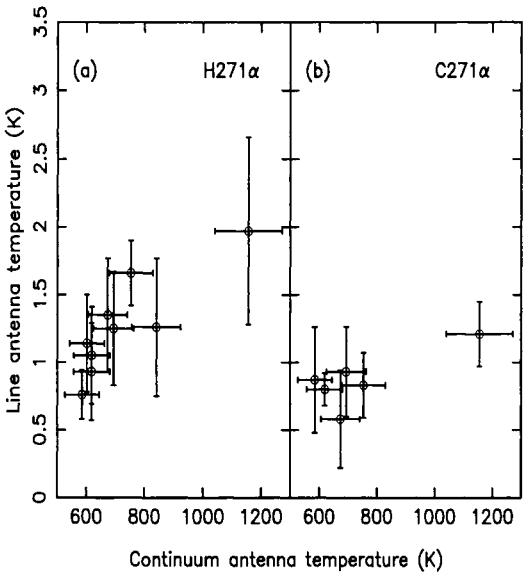

Figure 2. The line antenna temperatures observed at the nine positions are plotted against the continuum antenna temperatures measured at the corresponding positions: (a) for hydrogen (b) for carbon.

The observed line temperatures at the nine positions are plotted against the corresponding continuum temperatures in Fig. 2(a). There is a clear correlation with a correlation coefficient of 0.86. Since the continuum at this frequency is dominated by non-thermal emission, this correlation indicates that stimulated emission is dominant. The importance of stimulated emission of recombination lines at low frequencies towards the Galactic Centre was first noted by Pedlar et al. (1978).

3.1 Narrow and broad components in the hydrogen line

In Fig. 3(a), we show the integrated spectrum obtained by averaging the spectra from all the nine positions. The hydrogen line feature in the integrated spectrum seems to have a narrow component superimposed on a broad component. A two-component Gaussian fit gives a width of about 38 km s^{-1} for the broad feature and 8 km s^{-1} for the narrow feature. In this paper, we refer to features with linewidths less than 10 km s^{-1} as narrow components. The fitted parameters are given in Table 3. While the broad component could be attributed to a normal H II region along the line of sight, the

narrow component, if real, suggests interesting possibilities. The parameters of the emission region responsible for the broad component have been modelled previously by Pedlar et al. (1978), Hart & Pedlar (1980), Anantharamaiah & Bhattacharya (1986) and Anantharamaiah et al. (1990). This component will not be discussed further here. We just note here that based on the parameters of the H356α line near 145 MHz, which is the lowest frequency hydrogen recombination line observed in this direction, Anantharamaiah et al. (1990) have deduced that the electron density of the gas responsible for the low-frequency lines is $\sim 7\,\mathrm{cm}^{-3}$ with an emission measure of $\sim 2200\,\mathrm{pc\,cm}^{-6}$, assuming a temperature of $\sim$7500 K.

The narrow component was not detected in any of the earlier observations. At low frequencies, man-made narrow-band interferences can produce such spectral features. During the whole of our observing session the local standard of rest (LSR) velocity correction has changed by about $15\,\mathrm{km\,s}^{-1}$ and therefore any time-independent narrow-band interference at a constant frequency would have broadened out to at least $15\,\mathrm{km\,s}^{-1}$ when the spectra of all the positions were averaged. However, interferences can be time-dependent and we cannot therefore rule out with certainty that this feature is an artefact. Further observations are required to confirm this feature. Narrow hydrogen lines have in fact been detected in other directions in the Galaxy, and they are believed to originate either in partially ionized regions that are adjacent to normal H II regions (Pankonin et al. 1977; Roelfsema, Goss & Geballe 1989) or in cool H II regions with temperatures < 3000 K (Shaver, McGee & Pottasch 1979). Therefore we investigate whether a reasonable physical model can explain the observed line optical depth of the narrow feature near 328 MHz while being consistent with observations at other frequencies.

3.2 Is there a reasonable physical model for the narrow component?

If we regard the width of the narrow feature to be due to thermal motions alone, then an upper limit to the temperature of 1380 K is obtained. From considerations of pressure broadening, the maximum allowed value of electron density is 7.3 cm^{-3} if the temperature is as low as 200 K. In Figs 3(b) and (c), we show the averaged spectra of positions at positive Galactic longitudes and those at negative Galactic longitudes respectively. The presence of the narrow component in both these spectra indicates that the line-emitting region is at least 1° in extent along the direction of Galactic longitude. The angular resolution of the observation along the direction of Galactic latitude is $\sim 2°$ and hence the extent of the cloud in that direction is uncertain. We considered a homogeneous cloud with an angular size of $1° \times 1°$ and tried several models with different electron temperatures and densities. The emission measure that gives the observed H271α line optical depth for a given pair of T_e and n_e was first computed. Using these parameters, the expected optical depths at other frequencies in the range 75 MHz to 1 GHz were computed and compared with the available observations. The departure coefficients (b_n and β_n) were computed using the computer code of Salem & Brocklehurst (1979). Fig. 4 shows the plots of line optical depth as a function of principal quantum number for two models that fit the observations. Table 4 summarizes the parameters of two of the models. The last column in Table 4 gives the distance to the cloud estimated on the assumption that the cloud has similar dimensions both along the line of sight and perpendicular to it. The two curves in Fig. 4 are normalized to the line optical depth of the narrow component obtained in the present observation. The measured optical depths of the hydrogen lines at other frequencies are marked as upper limits after correcting for beam dilution.

The pathlength obtained for the low-temperature model is 0.1 pc and that for the higher temperature model (solid line) is 2.6 pc. Thus

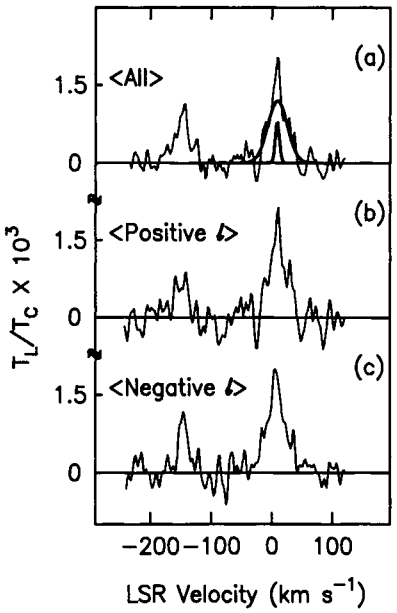

Figure 3. (a) The average spectrum obtained by integrating the spectra of all the nine positions. The two Gaussian profiles obtained from a two-component Gaussian fit to the hydrogen line are also shown. (b) and (c) Spectra obtained by averaging the observed spectra of positions corresponding to positive and negative longitudes respectively.

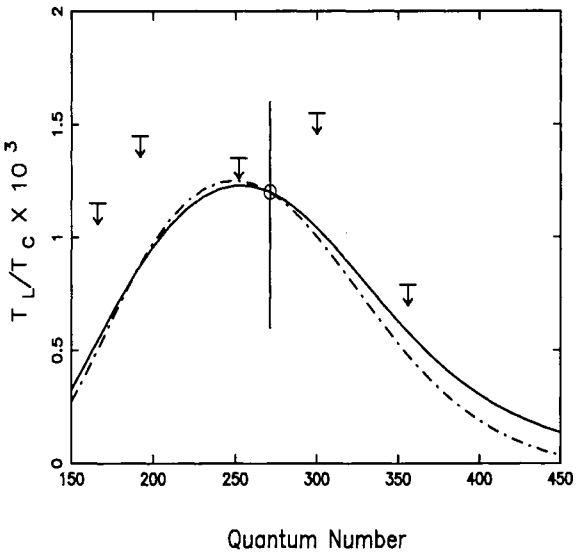

Figure 4. The hydrogen line optical depths computed for different models are plotted against principal quantum number. Model parameters are given in Table 4. The upper limits on optical depths at $n = 166$ and 192 are from Kesteven & Pedlar (1977), that at $n = 252$ is from Pedlar et al. (1978), that at $n = 300$ is from Casse & Shaver (1977) and that at $n = 356$ from Anantharamaiah et al. (1990). The measured optical depths are corrected for beam dilution. The solid curve corresponds to model (1) with $T_e = 1200$ K, $n_e = 1.5\,\mathrm{cm}^{-3}$ and $S = 2.6$ pc, and the dash–dotted curve corresponds to model (2) with $T_e = 100$ K, $n_e = 1.0\,\mathrm{cm}^{-3}$ and $S = 0.1$ pc.

Table 4. Model parameters for the narrow hydrogen.

Model	T_e (K)	n_e (cm^{-3})	EM (pc cm^{-6})	S (pc)	Distance (pc)
1	1200	1.5	5.9	2.6	149
2	100	1.0	0.1	0.1	5.7

there exist reasonable physical models for the narrow-line emission. Since the non-zero LSR velocities of the narrow and broad components are similar, it is possible that the narrow feature originates in a partially ionized outer envelope of the H II region which is responsible for the broad feature.

4 THE CARBON LINE

Carbon lines have been detected in positions 5 to 9 and also in position 3 (see Fig. 1). Table 2 gives the parameters of the detected carbon lines. The line-to-continuum ratio varies from 6.2×10^{-4} to 14.8×10^{-4} and seems to increase towards negative Galactic longitudes. The width of the line ranges from 10 to 26 km s^{-1}. The centroid velocities of all the lines, except that at position 5 (Galactic Centre), are positive and have a mean value of $\sim+3$ km s^{-1}. The mean centroid velocity of $+3$ km s^{-1} is less than the average LSR velocity of the hydrogen line detected in the same direction.

As in the case of the hydrogen line, the antenna temperature of the carbon line also shows a correlation with the continuum temperature (see Fig. 2b), implying that stimulated emission is dominant. Stimulated emission of carbon recombination lines near 325 MHz in the direction of Cas A has been demonstrated by Payne, Anantharamaiah & Erickson (1989).

The large extent of the carbon line emission region is evident from the detection of lines at various positions. Although the line is not seen in the spectra of positions 1, 2 and 4 (see Fig. 1), a weak and broad feature can be seen after smoothing the spectra to a velocity resolution of $\sim$10 km s^{-1}. It therefore appears that the line emission region is at least 1° in extent. The line-to-continuum ratio and the width of the lines detected at different positions can be considered to be a constant within the errors (see Table 2). The LSR velocity of the line, however, is not the same for all the positions. The parameters of the line feature estimated from the integrated spectrum are given in Table 3.

4.1 Likely site of carbon line emission

If the carbon line and the narrow hydrogen line originate from the same cloud, then they should have the same LSR velocity. Such system of lines have been observed in other sources in the Galaxy at frequencies higher than 1 GHz (e.g. Pankonin et al. 1977). The widths of the lines detected in such cases are quite small (<5 km s^{-1}). These lines have been interpreted as originating from C II zones adjacent to H II regions. Such an interpretation can be ruled out in the present case since the average width of the carbon line ($\sim$15 km s^{-1}) is greater than that of the narrow hydrogen line ($\sim$8 km s^{-1}), and the LSR velocity of the carbon line obtained from the integrated spectrum ($\sim$3 km s^{-1}) is different from that of the narrow hydrogen line ($\sim$9.3 km s^{-1}).

The other possibility, which seems more likely, is that the observed carbon line is the emission counterpart of the absorption recombination line observed near 75 MHz towards the Galactic Centre (Anantharamaiah et al. 1988; Erickson et al. 1995). The

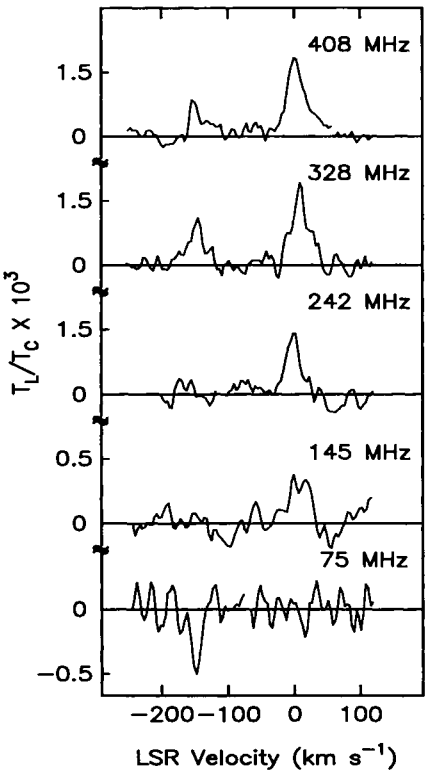

Figure 5. Recombination line spectra towards the Galactic Centre at different frequencies. The spectra at frequencies of 408 and 242 MHz are from Pedlar et al. (1978), that at 145 MHz is from Anantharamaiah et al. (1990), that at 75 MHz is from Anantharamaiah et al. (1988), and that at 328 MHz is from the present observation. The phenomenon of turnover of the carbon line from emission to absorption is clearly seen. Table 5 gives the observed parameters of the carbon line obtained from these spectra.

phenomenon of turnover of carbon recombination lines from absorption at low frequencies (< 100 MHz) to emission at higher frequencies (> 200 MHz) has been observed towards Cas A (Payne et al. 1989) and M16 (Anantharamaiah et al. 1988). We show, in Fig. 5, the recombination line spectra observed towards the Galactic Centre at five different frequencies below 500 MHz. It is clear that we are witnessing the same phenomenon of turnover from emission to absorption.

Two types of models have been considered for the low-frequency carbon recombination lines observed towards Cas A (Payne et al. 1989; Payne, Anantharamaiah & Erickson 1994). In the cold gas model, the carbon lines are supposed to originate in cold molecular clouds which have temperatures < 25 K and where carbon is ionized due to the background UV radiation. In this case, the population of high quantum number states of carbon is essentially controlled by hydrogenic-type recombination processes. In the warm gas model, the carbon lines are formed in relatively warm ($T\sim$50–100 K) H I clouds. At these temperatures, a dielectronic-like recombination process, first proposed by Watson et al. (1980), profoundly influences the population of high quantum number states in carbon. The carbon lines detected towards Cas A were found to have a spatial correspondence with the H I absorption observed in the same direction (Anantharamaiah et al. 1994). Payne et al. (1994) have examined various models to interpret the carbon lines observed in the direction of Cas A and found a consistent model which associates the carbon

Table 5. Observed parameters of the carbon line.

n	ΔV (FWHM) (km s^{-1})	$-\int \tau_L d\nu$ (s^{-1})	Beam size (°×°)	Ref.
166	(18)	< 16	0.37 × 0.37	1
252	12	14	0.7 × 0.7	2
271	17.5	17	1 × 2	3
300	(18)	< 7.0	1.2 × 1.2	2
356	(18)	< |2.0|	3.3 × 3.3	4
445	14.8	−2.0	6.7 × 6.7	5
445	24.0	−4.2	4.0 × 4.0	6

(1) Brown & Balick (1973); (2) Pedlar et al. (1978); (3) present observation; (4) Anantharamaiah et al. (1990); (5) Anantharamaiah et al. (1988); (6) Erickson et al. (1995).

line-emitting gas with H I clouds in the same direction. It is possible that the carbon line observed towards the Galactic Centre also originates in one or more H I clouds in the same direction. We note that the width (11.8 km s^{-1}) and centroid velocity (0.2 km s^{-1}) of the dominant 21-cm absorption feature (Radhakrishnan & Sarma 1980) are comparable to the corresponding parameters for the carbon line given in Table 3. On the assumption that the observed carbon line originates in H I clouds, we examine below models for the line-emitting region based on hydrogenic level populations as well as models that incorporate the effects of dielectronic-like recombination.

4.2 A model for the carbon line-emitting cloud

The parameters of the carbon line observed at different frequencies are summarized in Table 5. Based on the observation that the line-to-continuum ratios of the carbon line near 328 MHz are similar with telescope beams of 2° × 2° and 2° × 1° (Fig. 1), we consider a homogeneous cloud of angular size 2° lying in the direction of the Galactic Centre. The detection of the absorption line near 75 MHz with telescope beams of 4° (Erickson et al. 1995) and 6°.7 (Anantharamaiah et al. 1988) also indicates that the line-emitting region is quite extended. In the present analysis, we used the parameters of the carbon emission line obtained from the integrated spectrum (Fig. 3). For modelling, we computed the optical depth integrated over the frequency using the equation

$$\int \tau_L d\nu = 2.046 \times 10^6 \frac{EM}{T_e^{5/2}} \exp\left(\frac{1.58 \times 10^5}{n^2 T_e}\right) b_n \beta_n \mathrm{s}^{-1} \qquad (1)$$

(Payne et al. 1994). For the computation of departure coefficients, we used a non-thermal background temperature of 10^4 K at 100 MHz, with a spectral index of −2.7.

We tried several models with hydrogenic departure coefficients assuming different electron temperatures and densities. Almost all the models with reasonable combinations of T_e, n_e and EM fail to fit the observed variation of integrated optical depth with frequency. For example, a model with $T_e \sim 33$ K, $n_e \sim 2.5$ cm^{-3} and EM ~ 6.9 × 10^{-2} pc cm^{-6} is indeed consistent with all the observations below 500 MHz. The pathlength through the cloud is $\approx 10^{-2}$ pc, which suggests a thin sheet geometry since the angular extent of the cloud is 2°. If we assume that all the electrons are due to ionization of carbon and take the carbon depletion factor to be 0.5 and the abundance ratio C/H to be cosmic (4×10^{-4}), then the implied neutral hydrogen density in the cloud is 1.3×10^4 cm^{-3}. This density is at least an order of magnitude higher than typical densities in H I clouds. We therefore conclude that any model with only hydrogenic departure coefficients does not give a satisfactory fit to the data. We therefore turn to models that incorporate the dielectronic-like effects proposed by Watson et al. (1980).

The departure coefficients that include the effects of dielectronic-like recombination were calculated using the computer code of Walmsley & Watson (1982) which has been further modified by Payne et al. (1994). The carbon depletion factor for the calculation was taken to be 0.5. We tried several models with different electron temperatures and densities. Table 6 summarizes the parameters of four models. Fig. 6 shows the predicted integrated optical depth as a function of principal quantum number for the four model clouds. Models 1 (solid line), 2 (dashed curve) and 3 (dash–dot–dashed line) are consistent with all the observations except the 242-MHz upper limit. We found no model that can be consistent with the 242-MHz upper limit and other observations (see e.g. model 4 in Fig. 6). The deduced neutral hydrogen densities (see Table 6) in all three models are acceptable. However, model 2 can be ruled out since the effective pathlength required is larger than the pathlength through the Galaxy. Furthermore, the thermal pressure in model 2 (450 cm^{-3} K) is an order of magnitude lower than the typical interstellar pressure. Note that the effective pathlength deduced in these models and given in Table 6 need not correspond to a single continuous stretch along the line of sight. More likely, the effective pathlength represents a sum of the pathlengths through a large number of line-emitting clouds or regions along the line of sight. Assuming that the total extent of the interstellar medium (ISM) towards the Galactic Centre is ~20 kpc, the deduced line-of-sight filling factors of the clouds for the different models are given in Table 6.

The filling factors, the neutral hydrogen density and the pressure deduced for models 1 and 3 are remarkably similar to the corresponding values for the cold neutral component (i.e. neutral H I clouds or CNM) of the ISM (McKee & Ostriker 1977; see also Kulkarni & Heiles 1988). Thus our observations support the idea that the low-frequency carbon recombination lines arise in the neutral H I component of the ISM (Payne et al. 1989, 1994; Anantharamaiah et al. 1994). This association also provides a natural explanation for the observed width of the carbon line which is ~17.0 km s^{-1}. This width is much larger than the intrinsic width of individual clouds (~3 km s^{-1}). Since the

Table 6. Parameters from dielectronic models.

Model	T_e (K)	n_e (cm^{-3})	EM (pc cm^{-6} × 10^2)	S (kpc)	Filling factor	n_H (cm^{-3})	Pressure (cm^{-3} K)
1	80	0.007	2.5	0.5	0.03	35	2800
2	90	0.001	3.9	38.7	> 1.0	5	450.0
3	70	0.01	1.9	0.19	0.01	50	3500
4	200	0.005	13.2	5.3	0.3	25	5000

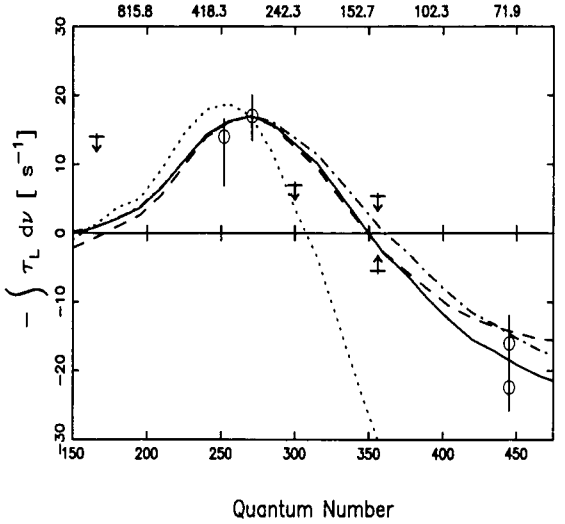

Figure 6. The optical depth of the carbon line integrated over the frequency as a function of principal quantum number is plotted for different models. The recombination line frequencies (in MHz) corresponding to different quantum numbers are marked on the top. The models take into account the effect of dielectronic-like recombination on the level populations. The model parameters are given in Table 6. The observed line parameters plotted here are from Table 5 and corrected for beam dilution. Model 1 (solid curve), 2 (dashed curve) and 3 (dash–dot–dashed curve) are consistent with all observations except the 242-MHz ($n = 300$) upper limit. Model 4 (dotted curve) is consistent with 242-MHz observations but predicts large optical depths at lower frequencies.

measured linewidth is nearly constant between 75 and 400 MHz (Table 5), it is clear that the linewidth is not dominated by pressure broadening. In the case of the 21-cm H I absorption towards the Galactic Centre, the observed linewidth of 11.8 km s^{-1} is attributed to random motions of a large number of clouds along the line of sight (Radhakrishnan & Sarma 1980). If the carbon recombination lines arise in these H I clouds then a similar width is expected for the carbon lines. Linewidths much larger than that expected for individual clouds were observed also by Erickson et al. (1995) in carbon recombination lines at 75 MHz towards several directions in the Galactic plane. Erickson et al. (1995) attributed these widths to a combination of Galactic rotation and random motions of the clouds. A similar explanation appears to hold good for the carbon lines observed here towards the Galactic Centre.

5 SUMMARY

In this paper we have described the observation and interpretation of H271α (328.5959 MHz) and C271α (328.7597 MHz) recombination lines towards the Galactic Centre region using the Ooty Radio Telescope. We observed nine positions around the Galactic Centre with an angular resolution of $2^\circ \times 6.2$ arcmin. Hydrogen lines were detected in all the positions and carbon lines in at least six of them. A strong correlation of the observed line strength with the background non-thermal continuum emission indicates that stimulated emission is dominant for both the lines.

In the spectrum obtained by averaging the spectra of all the nine positions, the hydrogen line shows a narrow and a broad feature. The properties of the cloud emitting the broad component are consistent with a line-of-sight low-density H II region. Further observations are required to confirm the narrow feature. If the narrow feature is real, it can originate in a region with physical properties $T_e \sim 100$–1200 K, $n_e \sim 1.0$–1.5 cm^{-3} and an effective pathlength of ~0.1–2.6 pc.

The observed carbon lines appear to be the emission counterpart of the absorption lines detected at frequencies less than 100 MHz in the direction of the Galactic Centre. Such absorption lines are believed to be associated with H I clouds. The parameters of the 21-cm H I absorption line, observed towards the Galactic Centre, show good agreement with the carbon line parameters. We find that the models that incorporate hydrogenic departure coefficients do not explain the recombination line data satisfactorily. Models that take into account the dielectronic-like recombination process in the computation of the level population of carbon atoms are more consistent with the observations. The physical properties obtained in this model are close to the typical values for H I clouds. On the basis of thermal pressure and filling factor arguments we have selected models with $T_e \sim 70$–80 K, $n_e \sim 0.005$–0.01 cm^{-3} and an effective pathlength of 200–500 pc. The deduced effective pathlength corresponds to a filling factor comparable to that of the cold neutral component of the ISM.

ACKNOWLEDGMENTS

We thank T. Velusamy and V. Balasubramanian for many useful discussions and for providing telescope time and technical help for these observations. DAR thanks the Raman Research Institute for generously allowing him to use their research facilities. This paper is based on part of the MSc thesis of DAR, submitted to the University of Poona. An error in the thesis regarding the estimation of the pathlengths required for dielectronic models for the carbon line emission has been corrected in this paper. We thank Nimisha G. Kantharia for pointing out the error.

REFERENCES

Anantharamaiah K. R., Bhattacharya D., 1986, JA&A, 7, 141
Anantharamaiah K. R., Yusef-Zadeh F., 1988, in Morris M., ed., Proc. IAU Symp. 136, The Center of the Galaxy. Kluwer, Dordrecht, p. 159
Anantharamaiah K. R., Payne H. E., Erickson W. C., 1988, MNRAS, 235, 151
Anantharamaiah K. R., Payne H. E., Bhattacharya D., 1990, in Gordon M. A., Sorochenko R. L., eds, Radio Recombination Lines: 25 years of investigation. Kluwer, Dordrecht, p. 259
Anantharamaiah K. R., Erickson W. C., Payne H. E., Kantharia N. G., 1994, ApJ, 430, 682
Brown R. L., Balick B., 1973, ApJ, 185, 843
Casse J. L., Shaver P. A., 1977, A&A, 61, 805
Erickson W. C., McConnell D., Anantharamaiah K. R., 1995, ApJ, 454, 125
Hart L., Pedlar A., 1980, MNRAS, 193, 781
Kesteven M. J., Pedlar A., 1977, MNRAS, 180, 731
Kulkarni S. R., Heiles C., 1988, in Verschuur G. H., Kellermann K. I., eds, Galactic and Extragalactic Radio Astronomy. Springer-Verlag, Berlin, p. 95
McKee C. F., Ostriker J. P., 1977, ApJ, 196, 565
Pankonin V., Walmsley C. M., Wilson T. L., Thomasson P., 1977, A&A, 57, 341
Payne H. E., Anantharamaiah K. R., Erickson W. C., 1989, ApJ, 341, 890
Payne H. E., Anantharamaiah K. R., Erickson W. C., 1994, ApJ, 430, 690
Pedlar A., Davies R. D., Hart L., Shaver P. A., 1978, MNRAS, 182, 473
Radhakrishnan V., Sarma N. V. G., 1980, A&A, 85, 249

Rodriguez L. F., Chaisson E. J., 1979, ApJ, 228, 734
Roelfsema P. R., Goss W. M., 1992, A&AR, 4, 161
Roelfsema P. R., Goss W. M., Geballe T. R., 1989, A&A, 222, 247
Salem M., Brocklehurst M., 1979, ApJS, 39, 633
Shaver P. A., 1975, Pramana, 5, 1
Shaver P. A., McGee R. X., Pottasch S. R., 1979, Nat, 280, 476
Walmsley C. M., Watson W. D., 1982, ApJ, 260, 317
Watson W. D., Western L. R., Christensen R. B., 1980, ApJ, 240, 956

This paper has been typeset from a TEX/LATEX file prepared by the author.